REPORT DOCUMENTATION PAGE

Form Approved OMB No. 0704-0188

1. REPORT DATE *(DD-MM-YYYY)*	2. REPORT TYPE	3. DATES COVERED *(From – To)*
01-09-2003	Final Report	3 September 2002 - 02-Sep-03

4. TITLE AND SUBTITLE

Electrochemical synthesis of carbon nano- and microtubes from molten salts

5a. CONTRACT NUMBER
FA8655-02-M4076

5b. GRANT NUMBER

5c. PROGRAM ELEMENT NUMBER

6. AUTHOR(S)

Professor George Kaptay

5d. PROJECT NUMBER

5d. TASK NUMBER

5e. WORK UNIT NUMBER

7. PERFORMING ORGANIZATION NAME(S) AND ADDRESS(ES)
University of Miskolc
Egyetemvaros
Miskolc 3525
Hungary

8. PERFORMING ORGANIZATION REPORT NUMBER
N/A

9. SPONSORING/MONITORING AGENCY NAME(S) AND ADDRESS(ES)

EOARD
PSC 802 BOX 14
FPO 09499-0014

10. SPONSOR/MONITOR'S ACRONYM(S)

11. SPONSOR/MONITOR'S REPORT NUMBER(S)
SPC 02-4076

12. DISTRIBUTION/AVAILABILITY STATEMENT

Approved for public release; distribution is unlimited.

13. SUPPLEMENTARY NOTES

20040210 123

14. ABSTRACT

This report results from a contract tasking University of Miskolc as follows: The objective of the research project is to produce carbon nanotubes using molten salt electrolysis. A series of experiments will be performed to determine the relationship between production conditions and morphology of carbon tubes. Potential, current density, duration, and electrolysis mode will be varied in different experiments. The experiments will be performed in a sealed high temperature cell, under argon atmosphere. The resulting carbonaceous material will be characterized using mainly scanning electron microscopy (SEM) and atomic force microscopy (AFM).

15. SUBJECT TERMS
EOARD, Materials, Nanotechnology, Carbon nanomaterials

16. SECURITY CLASSIFICATION OF:			17. LIMITATION OF ABSTRACT	18, NUMBER OF PAGES	19a. NAME OF RESPONSIBLE PERSON
a. REPORT	b. ABSTRACT	c. THIS PAGE			CHARLES H. WARD, Lt Col, USAF
UNCLAS	UNCLAS	UNCLAS	UL	29	19b. TELEPHONE NUMBER *(Include area code)* +44 (0)20 7514 3154

Standard Form 298 (Rev. 8/98)
Prescribed by ANSI Std. Z39-18

Final (12 months) report for the project

"Electrochemical synthesis of carbon nano- and micro-tubes from molten salts"

performed against the Purchase Order Number FA8655-02-M4076
issued by European Office of Aerospace Research and Development (EOARD)
effective September 3, 2002

by the team led by Prof. George Kaptay
Department of Physical Chemistry,
University of Miskolc,
Miskolc-Egyetemváros,
Hungary, 3515

on September 1, 2003

delivered by e-mail to:
Charles H. Ward, Lt. Col., USAF,
Ms. Beth Wann, Contracting Officer

Project participants:
Prof. Dr. G. Kaptay (project leader, University of Miskolc)
Prof. Dr. E. Kálmán (sub-project leader, REC-HAS, Budapest)
J. Sytchev, Ph.D. student (electrolysis, cyclic voltammetry measurements)
M.S. Yaghmaee, junior lecturer (cleaning procedure, micro-tube evaluation)
N. Borisenko, 5th year undergraduate (cyclic voltammetry)
Z. Demeter, 3rd year undergraduate (cleaning procedure)
Dr. P. Nagy, research fellow (AFM)
T. Gábor, Ph.D. student (AFM)
A. Kovács, engineer (SEM)

(1) In accordance with Defense Federal Acquisition Regulation 252.227-7036, Declaration of Technical Data Conformity (Jan 1997),

"The Contractor, University of Miskolc, hereby delcares that, to the best of its knowledge and belief, the technical data delivered herewith under Contract No. FA8655-02-M4076 is complete, accurate, and complies with all requirements of the contract.

DATE: __15th October, 2003_____

Name and Title of Authorized Official: _dr. George Kaptay, Professor

(2) In accordance with the requirements in Federal Aquisition Regulation 52.227-13, Patent Rights—Acquisition by the *U.S.* Government (Jun 1989), *PLEASE SELECT **ONE** OF THE FOLLOWING STATEMENTS & DELETE THE OTHER:*

(B) "I certify that there were no subject inventions to declare as defined in FAR 52.227-13, during the performance of this contract."

DATE: **15th October, 2003**_____

Name and Title of Authorized Official: _ dr. George Kaptay, Professor

1. Introduction

Carbon nano-tubes were discovered in 1991 and since then different techniques to produce them have been studied. One of the possibilities is to obtain carbon nano/micro-tubes by electrochemical synthesis from molten salts using graphite cathode and a salt from which an alkali or alkaline earth metal can be deposited onto the surface of the cathode. According to our present understanding, the deposited alkali (Li, Na) or alkaline earth (Mg, Ca) atoms intercalate into the space between the graphite planes causing mechanical stress, and part of the depleting graphite planes appear to be in the form of carbon tubes. The typical diameter of those tubes ranges from 2 nanometers to 20 micrometers with a length being much larger than the actual diameter.

Our work for the duration of this project was twofold:

i. we carried out a series of cyclic voltammetry experiments in order to gain some basic understanding of the mechanism of nano-tube formation, or at least of its presumed first step: intercalation of deposited alkali/alkaline earth metals into graphite;

ii. we carried out a series of electrolysis experiments with the aim to produce carbon nano-tubes and micro-tubes, and analyzed the product by SEM (Scanning Electron Microscopy) and AFM (Atomic Force Microscopy).

According to the above, this report will have two chapters.

Chapter 1. The results of cyclic voltammetry experiments

According to our preliminary studies, LiCl, NaCl, $MgCl_2$ and $CaCl_2$ seem to be suitable molten salts for nano-tube synthesis. The reason for that is that electrolyzing these salts (or their mixtures), Li, Na, Mg or Ca atoms can be deposited on a graphite cathode, and they are all capable to intercalate in between the graphite planes. The goal of this sub-project is to gain some understanding of the mechanism of intercalation and thus nano-tube formation. In order to 'catch' the electrochemical signature of the intercalation process, we have performed the comparative electrochemical analysis of the NaCl (sodium chloride) and LiCl (lithium chloride) melts using method of cyclic voltammetry on the following three working electrodes:

i. Mo (molybdenum), having practically zero mutual solubility and no compound formation tendency with Na (or with NaCl), and thus serving as a 'reference' inert electrode;

ii. GC (glassy carbon), providing carbon sites for the deposited sodium and lithium, but not allowing intercalation of Na (Li) into its bulk – thus, the glassy carbon electrode can be considered as an 'intermediate reference' electrode between molybdenum and graphite electrodes;

iii. ' graphite working electrode, being the target material of our investigation.

Working with molten lithium chloride, it was found that molybdenum being in the melt undergoes corrosion, which is probably due to the traces of water present in the melt (unfortunately, it is very hard do remove water entirely from LiCl). So we decided to use steel instead of molybdenum for the investigation of molten LiCl.

In our previous report we have stated that voltammetry experiments will be performed for the $MgCl_2$ and $CaCl_2$ systems. However, we were unable to obtain reliable results for the magnesium chloride melt. Magnesium chloride as well as lithium chloride is known to be hygroscopic, forming the $MgCl_2 \cdot 6H_2O$ crystalline hydrate. The latter is decomposed when heated according to the following reaction:

$$MgCl_2 \cdot 6H_2O \rightarrow MgO + 2HCl\uparrow + 5H_2O\uparrow$$

Despite all precautions taken when preparing the salt for the experiment, this was probably the case. The crystalline hydrate decomposed releasing hydrogen chloride and water that caused

very intensive corrosion of the reactor material. Due to this, the electrolyte (that is, molten $MgCl_2$) became so badly contaminated by the corrosion products that it was impossible to obtain reliable voltammetric curves. For this reason the results on the magnesium chloride melt are not presented here. The voltammetry investigation of the calcium chloride melt is in progress.

1.1. Experimental

Cyclic voltammetry experiments were performed using a three-electrode electrochemical cell. To take voltammograms in the sodium chloride melt, a molybdenum wire (0.9 mm diameter, 0.29 cm^2 of active surface), glassy carbon rod (1.8 mm in diameter, 0.20 cm^2 of active surface) and graphite rod (3 mm in diameter, 0.47 cm^2 of active surface) were used as the working electrode (WE) in different experiments. The reference electrode was a molybdenum wire (0.9 mm in diameter).

We applied a steel wire (1.8 mm in diameter, 0.41 cm^2 of active surface) as the working and a glassy carbon rod (2.6 mm in diameter) as the reference electrode to take voltammograms in molten lithium chloride. The glassy carbon reference electrode was used in all experiments of the series.

A glassy carbon crucible was used as container for the electrolyte and also as the auxiliary electrode. The electrochemical experiments were carried out in a water-cooled nickel super-alloy reactor, placed inside a vertical tube furnace.

The temperature of experiment was 850°C and 700°C for sodium chloride and lithium chloride respectively. 50 cm^3 of salt (calculated for the respective working temperature) was placed in the glassy carbon crucible and flushed with dry Ar at room temperature. The salt was prepared by slow heating up to 120°C in vacuum and held at these conditions for around 40 h. After that the salt has been slowly heated up to 300°C, flushed with dry Ar, vacuumed and held at this temperature for 1h.

It is known that lithium chloride is able to attract and retain water even at high temperatures, so to remove as much water from it as possible, the salt was heated up to 500°C in vacuum and kept at this temperature for an hour. During this period, the system was flushed several times with argon to ensure the water removal. The same procedure was repeated at 600°C.

Then, the salt was heated up to the working temperature of 850°C (700°C for LiCl) in dry Ar, and held at this temperature over 1 h before starting the measurements. The electrochemical measurements were conducted by a computer-controlled potentiostat VoltaLab PGZ 301.

As alkali metals are known to dissolve in their molten chlorides, special care was taken to obtain reproducible and comparable results on all electrodes. As approximately 100 voltammetric curves were recorded in each experiment, the sequence of these curves was kept identical, and designed in a way to ensure that the electrolyte becomes saturated with the alkali metal as late as possible. Therefore, fast measurements with relatively positive break potential were conducted first, depositing a small amount of sodium (lithium). Curves were recorded in the following sequence:

i. according to the polarization rate: 20, 10, 3, 1, 0.3, 0.1, 0.03, 0.01 V/s (20 V/s is the maximum polarization rate allowed by the potentiostat);
ii. according to the break potential: for sodium chloride (reference electrode - Mo): 0, -0.2, -0.5, -0.75, -1.0, -1.25, -1.5, -1.6, -1.7, -1.8, -1.9 and –2.0 V; for lithium chloride (reference electrode – glassy carbon): -0.5, -0.75, -1.0, -1.25, -1.5, -1.6, -1.7, -1.8, -1.9, –2.0, -2.1, -2.2 and –2.3 V.

Each cyclic voltammogram was started at +0.2 V (-0.4 V for LiCl), conducted to the break potential and reversed to the initial potential. Depending on the rate of polarization and on the working electrode used, some of the voltamograms could not be fully recorded, as the current overload occurred (the value of current exceeded the limit of 1 A allowed by the potentiostat).

After each voltammogram a chronoamperogram was recorded, i.e. the current was measured as a function of time for 1–5 minutes until the remaining current became stable and low.

1.2. Experimental results

1.2.1. Results obtained for sodium chloride

Some characteristic voltammograms recorded at polarization rates of 10 V/s, 1 V/s and 0.1 V/s on the 3 working electrodes at a break potential of –1.5 V are presented in Figures 1-9. For the first look at the voltammograms, it is obvious that the anodic charge transfer is much less than the cathodic charge transfer. In other words, part of the deposited metal is not oxidized back in the same amount in the anodic cycle. This can be due to the escape of metallic sodium from the cathode surface due to its diffusion to the bulk of the electrolyte or to the bulk of the cathode, i.e. due to its intercalation into graphite. As the latter is the process to be studied by us, this deviation was studied in details.

The "loop" in Fig. 3 (the current after potential reversal and until approximately –1.3 V has more negative values than before potential reversal) may be due to the formation of a new phase (that is, sodium metal). This assumption is supported by quite a high value of the quantity of electricity (2.934 Coulomb) passed through the system when taking the curve.

The loops in Figs. 4 and 7 can be explained in the following way. At high polarization rates (1 V/s and higher) the system cannot follow the changes in the working electrode potential, which means that sodium ions cannot momentarily change the movement direction when the polarization is reversed. So for some time after the polarization is reversed we have increasing by absolute value flux of sodium ions, which causes the loop to appear. And the higher the polarization rate and negative break potential are the more pronounced this effect is.

The "wavy" appearance of the curve in Fig. 9 may be due to changes in the surface state of the working electrode because this curve was taken in the middle of the experiment and significant amounts of sodium might have adsorbed/desorbed on the electrode surface or, intercalated into the graphite lattice.

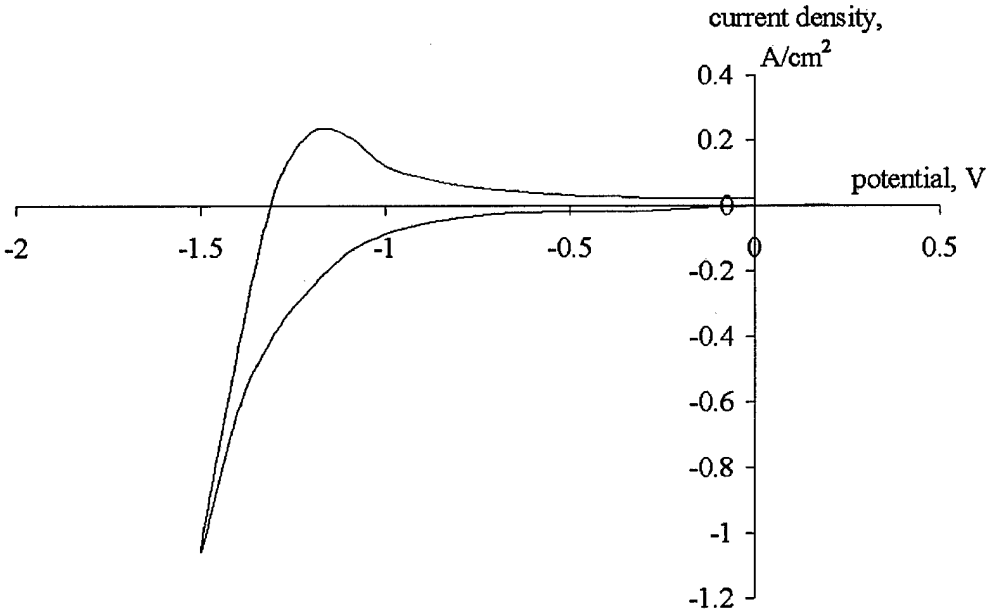

Fig. 1. Cyclic voltammogram recorded on a Mo electrode at a break potential of –1.5 V (Reference electrode - Mo). Polarization rate – 10 V/s, pure NaCl at 850°C.

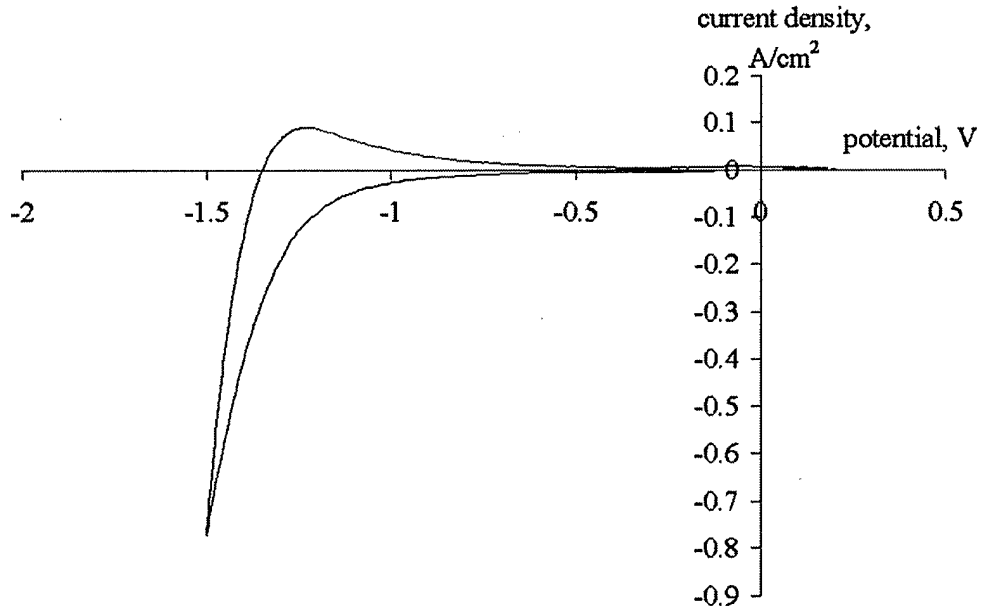

Fig. 2. Cyclic voltammogram recorded on a Mo electrode at a break potential of –1.5 V (Reference electrode - Mo). Polarization rate – 1 V/s, pure NaCl at 850°C.

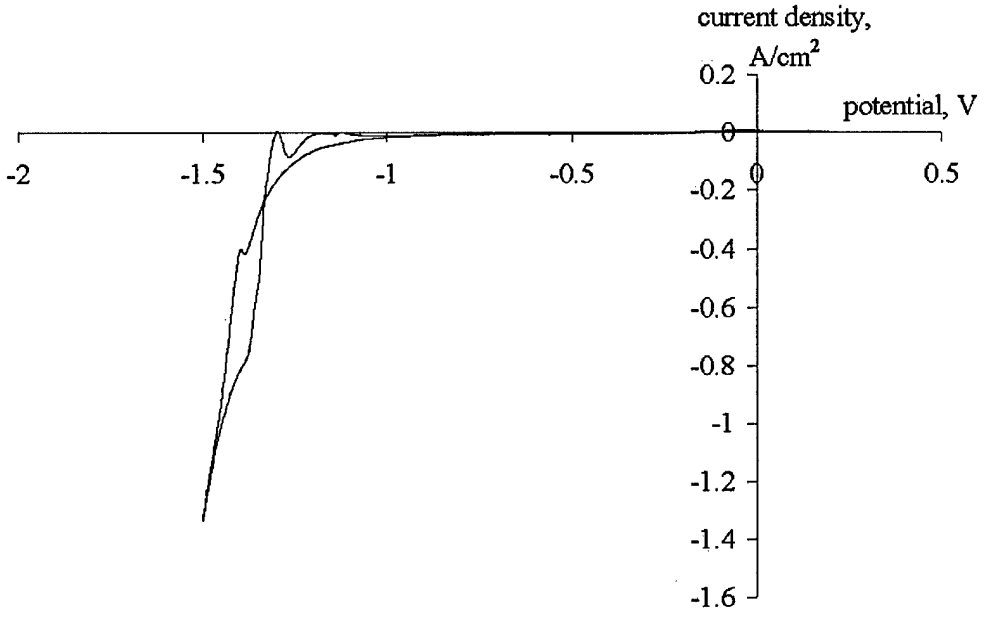

Fig. 3. Cyclic voltammogram recorded on a Mo electrode at a break potential of –1.5 V (Reference electrode - Mo). Polarization rate – 0.1 V/s, pure NaCl at 850°C.

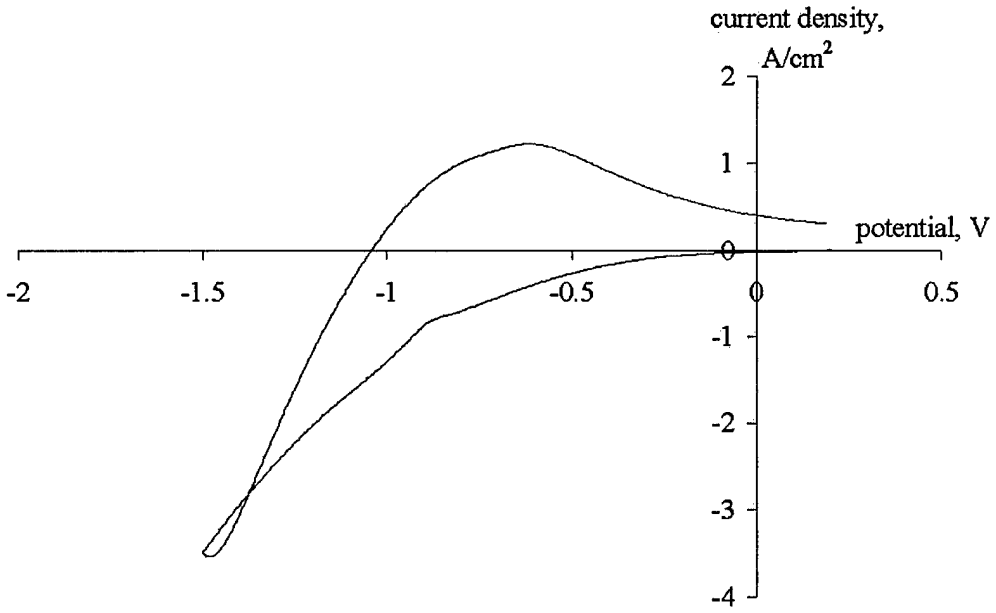

Fig. 4. Cyclic voltammogram recorded on a GC electrode at a break potential of –1.5 V (Reference electrode - Mo). Polarization rate – 10 V/s, pure NaCl at 850°C.

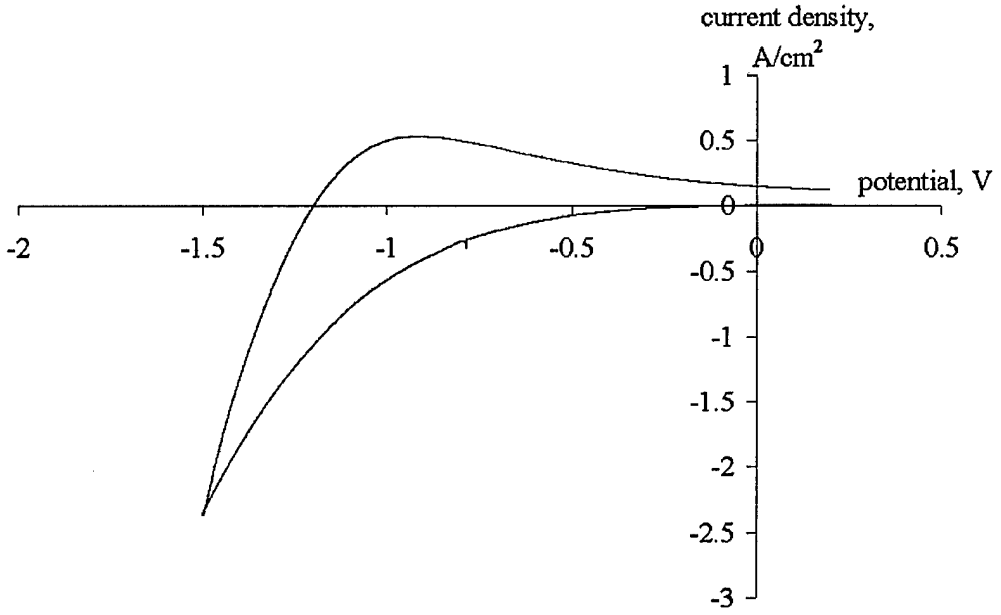

Fig. 5. Cyclic voltammogram recorded on a GC electrode at a break potential of –1.5 V (Reference electrode - Mo). Polarization rate – 1 V/s, pure NaCl at 850°C.

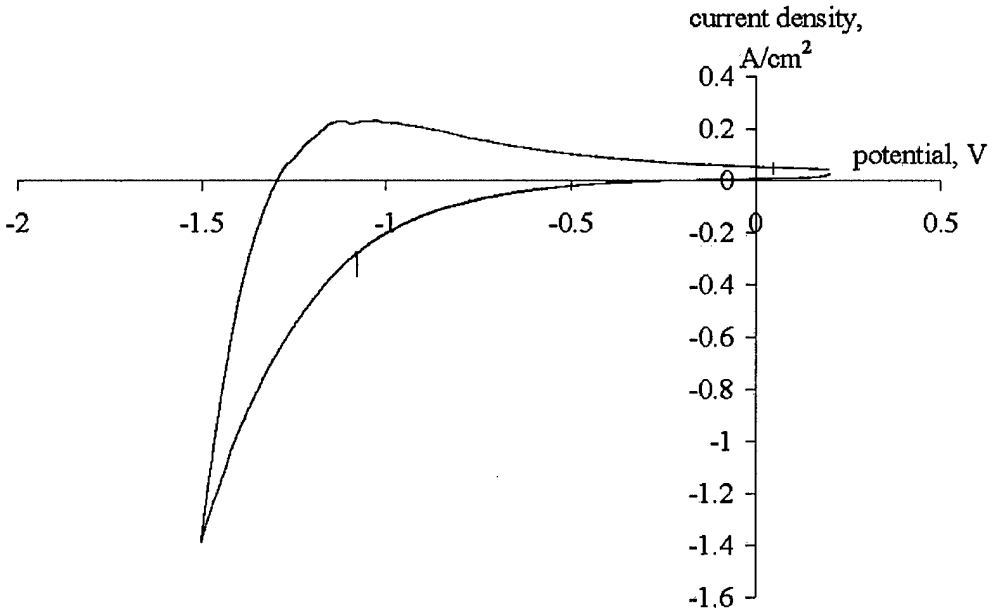

Fig. 6. Cyclic voltammogram recorded on a GC electrode at a break potential of –1.5 V (Reference electrode - Mo). Polarization rate – 0.1 V/s, pure NaCl at 850°C.

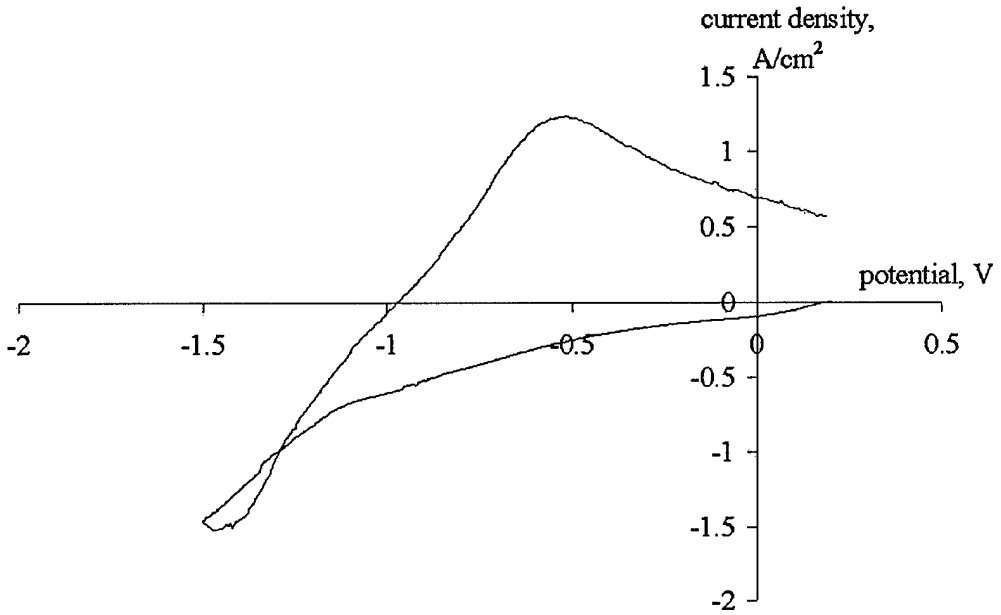

Fig. 7. Cyclic voltammogram recorded on a graphite electrode at a break potential of –1.5 V (Reference electrode - Mo). Polarization rate – 10 V/s, pure NaCl at 850°C.

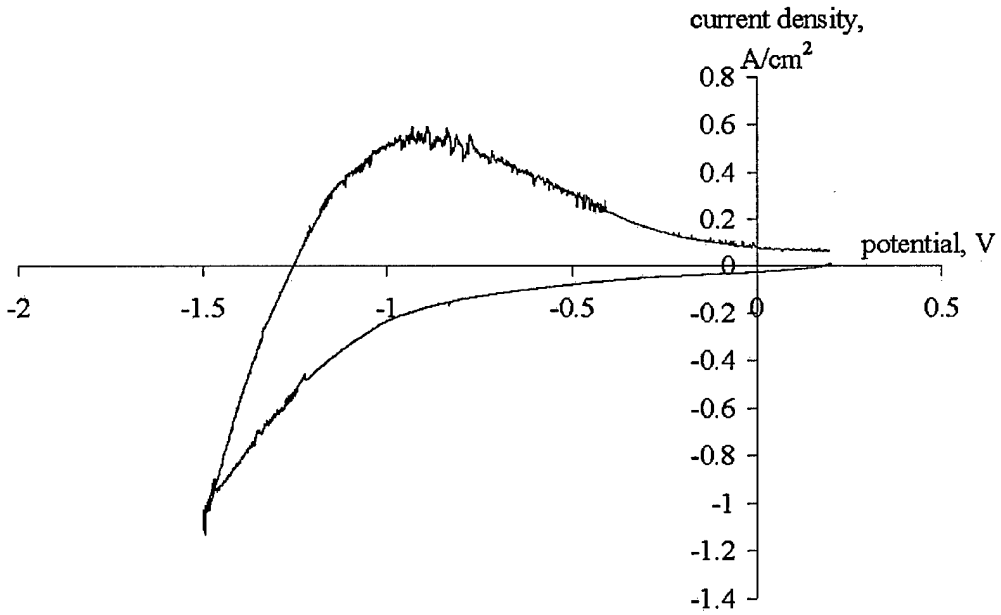

Fig. 8. Cyclic voltammogram recorded on a graphite electrode at a break potential of –1.5 V (Reference electrode - Mo). Polarization rate – 1 V/s, pure NaCl at 850°C.

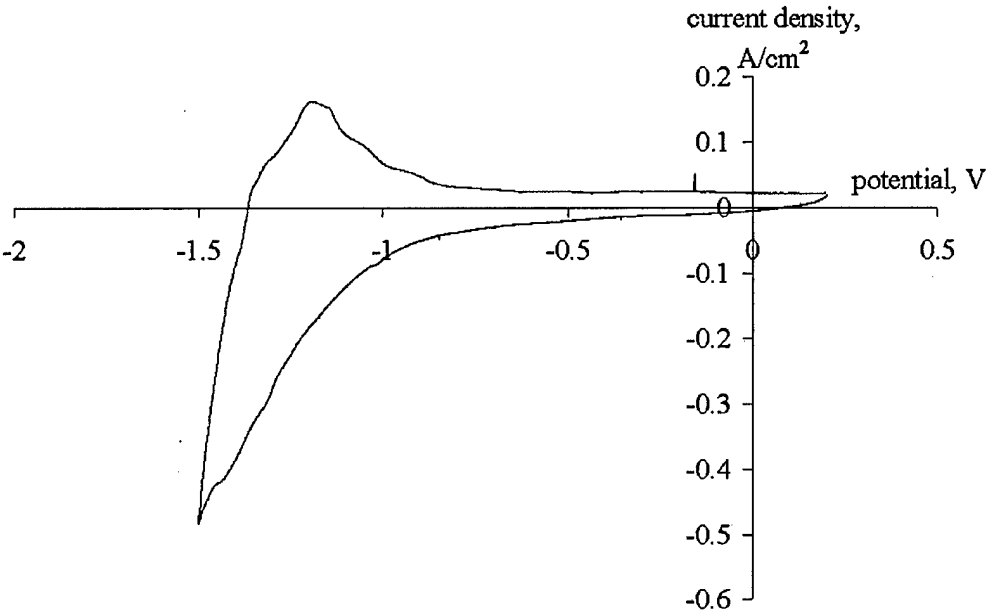

Fig. 9. Cyclic voltammogram recorded on a graphite electrode at a break potential of –1.5 V (Reference electrode - Mo). Polarization rate – 0.1 V/s, pure NaCl at 850°C.

1.2.2. Results obtained for lithium chloride

Some characteristic voltammograms recorded in the lithium chloride melt at polarization rates of 1 V/s and 0.1 V/s at a break potential of –2.2 V on the steel and at 10 V/s, 1 V/s and 0.1 V/s on the glassy carbon and graphite working electrodes at a break potential of –1.6 V are presented in Figures 10-17. As can be seen from Figs. 10 and 11, the reduction process of lithium ions on steel, which is inert towards lithium metal, takes place at -1.8-2.1 V versus the potential of the glassy carbon reference electrode. One can find that there is no such drastic difference between the cathodic and anodic charge transfers as it was in the case of the sodium chloride melt. However, the voltammograms taken on the glassy carbon and graphite electrodes (Figs. 12-17) differ principally from those obtained using the steel electrode. One can see that the cathodic current starts to rise as soon as we begin polarization of the electrode, and it is practically impossible to say when lithium reduction with the formation of metallic lithium phase on the electrode surface actually begins. The ratio between the cathodic and anodic charge transfers (or more precisely between the areas under the cathodic and anodic parts of voltammograms) varies depending on the polarization rate. At a polarization rate of 10 V/s the area under the cathodic parts of voltammograms is significantly larger than under the anodic parts. But at lower polarization rates this difference is not so big. The reason for the "wavy" appearance of the curve in Fig. 17 is probably the same as it was in the case of the sodium chloride melt: the voltammogram was taken in the middle of the experiment and quite a large amount of lithium might have adsorbed/desorbed on the electrode surface or intercalated into the graphite. In other words, the surface state of the electrode might have changed by the time the curve was taken.

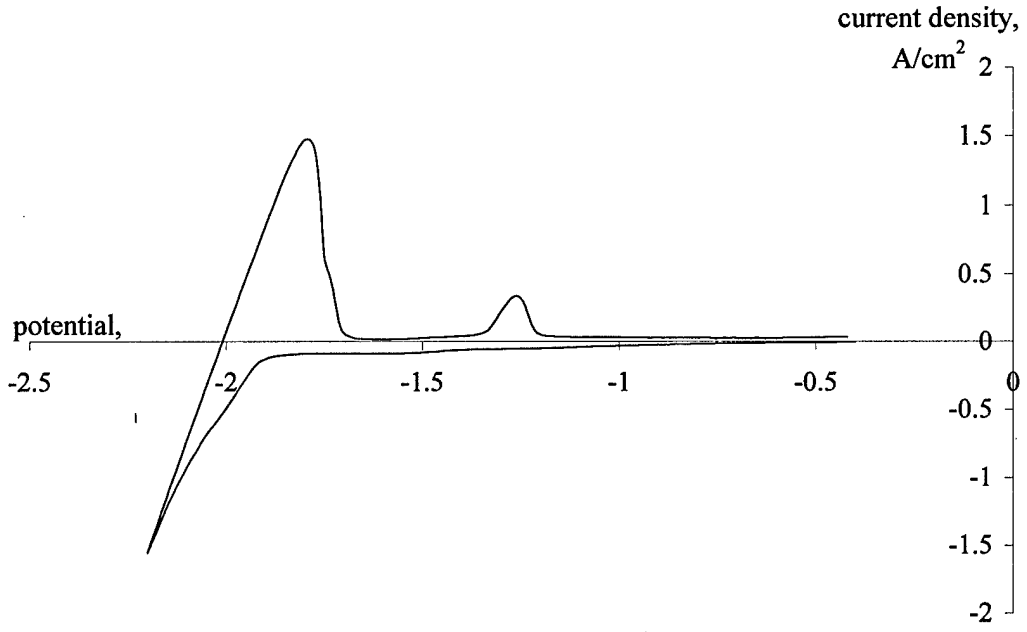

Fig. 10. Cyclic voltammogram recorded on a steel electrode at a break potential of –2.2 V (Reference electrode – glassy carbon). Polarization rate – 1.0 V/s, pure LiCl at 700°C.

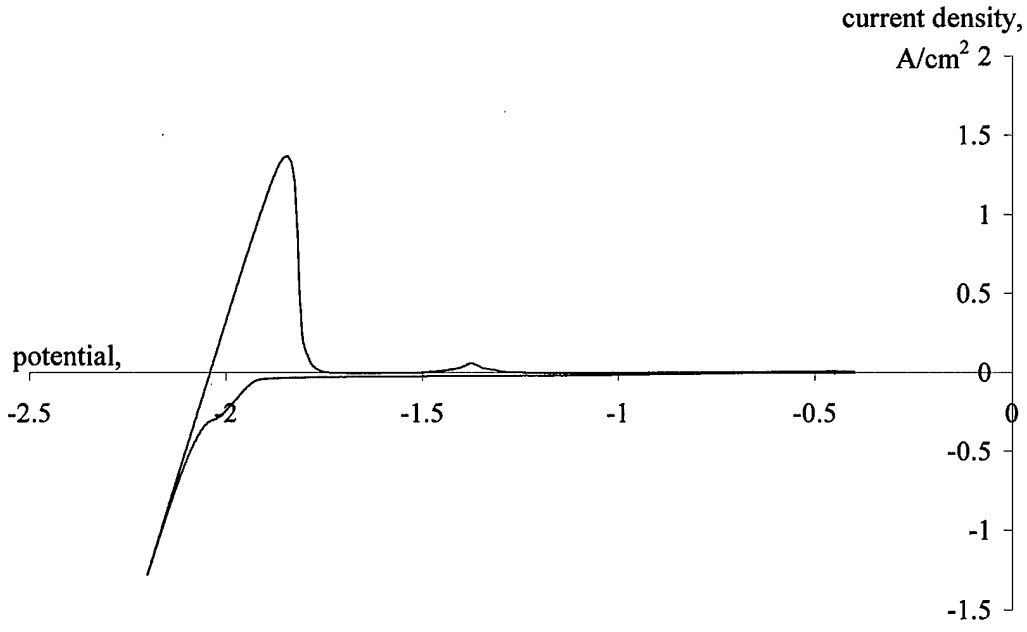

Fig. 11. Cyclic voltammogram recorded on a steel electrode at a break potential of –2.2 V (Reference electrode – glassy carbon). Polarization rate – 0.1 V/s, pure LiCl at 700°C.

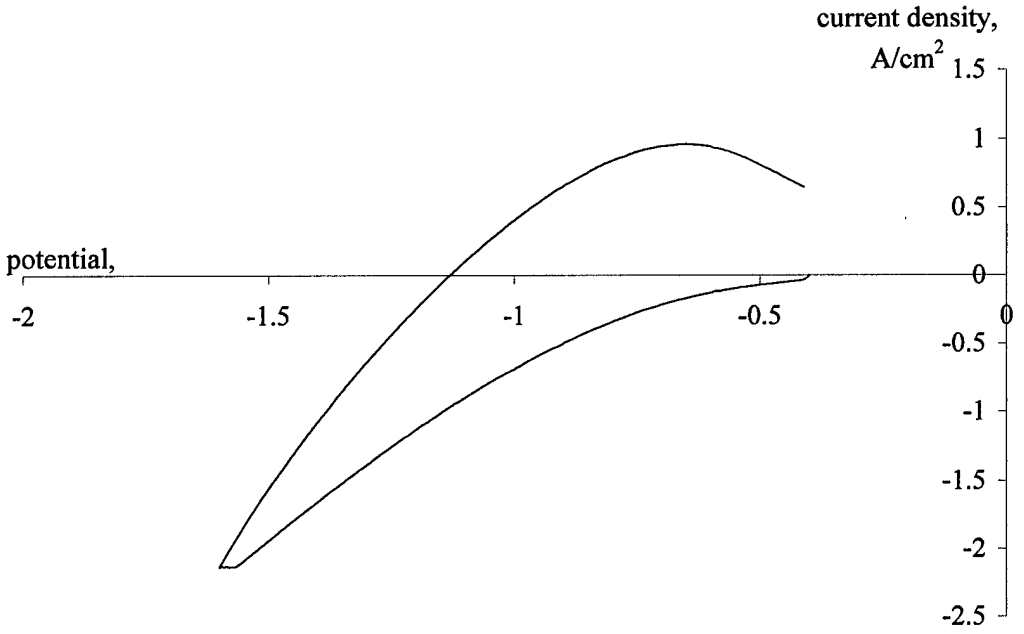

Fig. 12. Cyclic voltammogram recorded on a GC electrode at a break potential of –1.6 V (Reference electrode – glassy carbon). Polarization rate – 10 V/s, pure LiCl at 700°C.

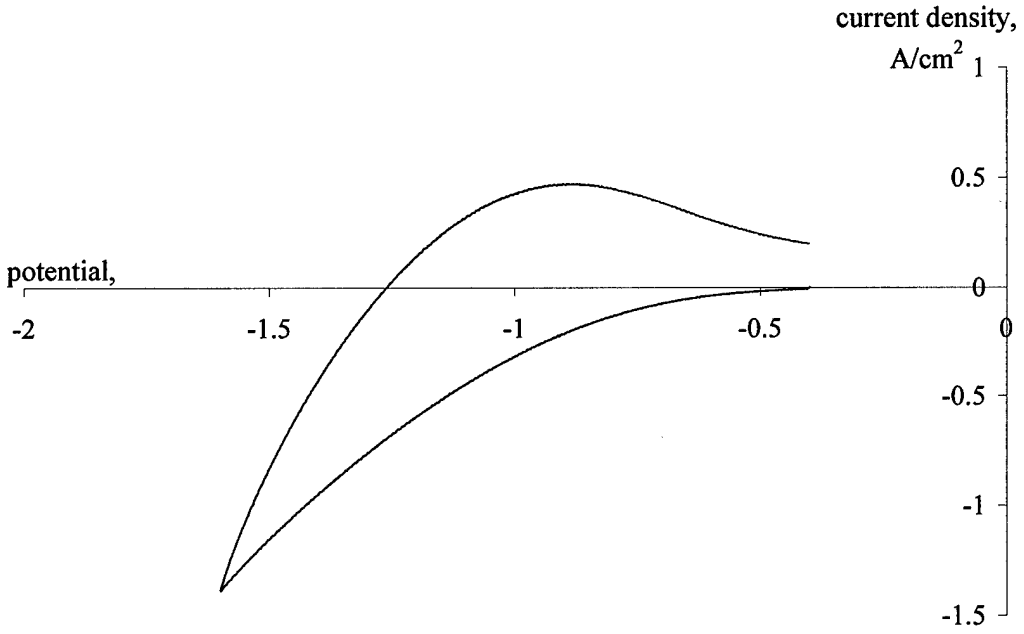

Fig. 13. Cyclic voltammogram recorded on a GC electrode at a break potential of –1.6 V (Reference electrode – glassy carbon). Polarization rate – 1 V/s, pure LiCl at 700°C.

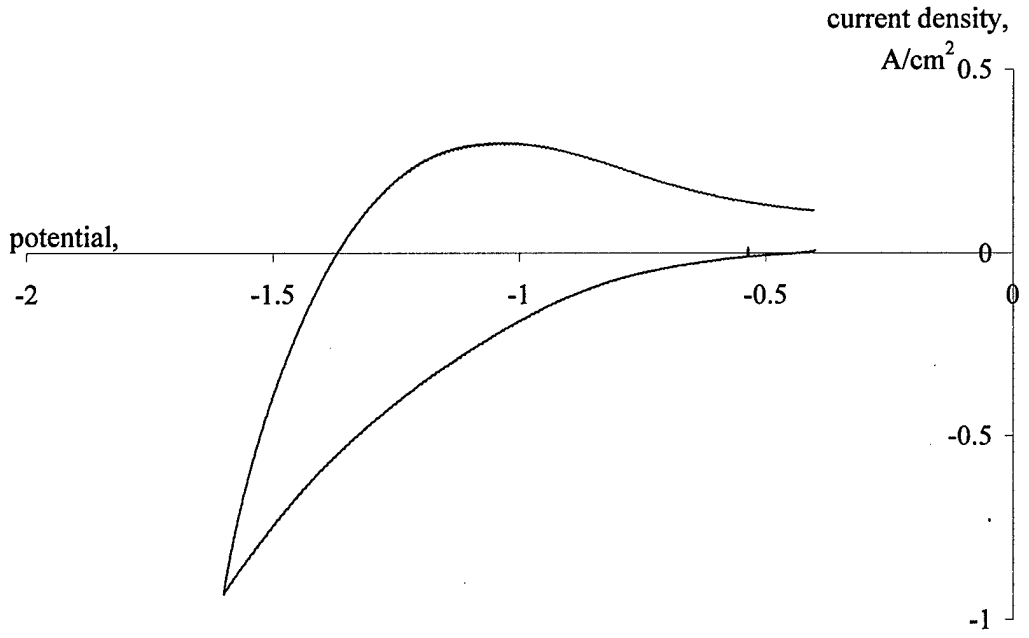

Fig. 14. Cyclic voltammogram recorded on a GC electrode at a break potential of –1.6 V (Reference electrode – glassy carbon). Polarization rate – 0.1 V/s, pure LiCl at 700°C.

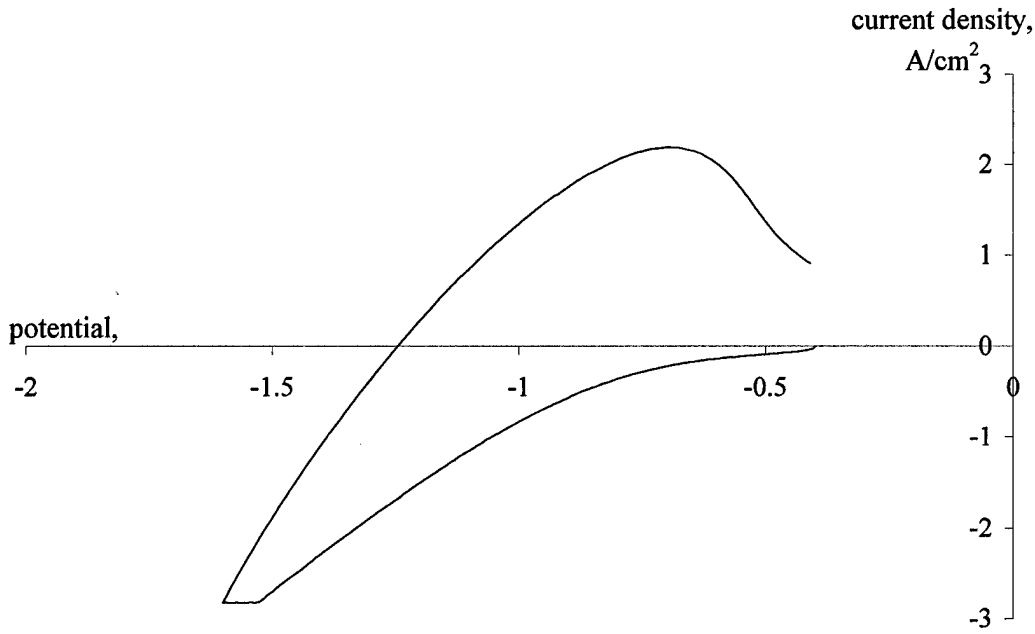

Fig. 15. Cyclic voltammogram recorded on a graphite electrode at a break potential of –1.6 V (Reference electrode – glassy carbon). Polarization rate – 10 V/s, pure LiCl at 700°C.

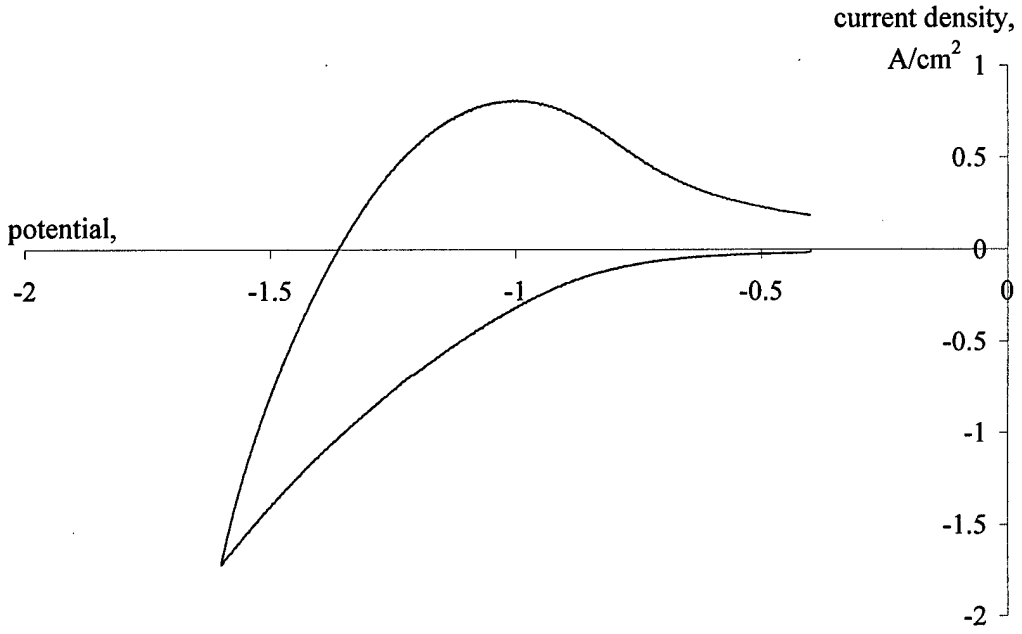

Fig. 16. Cyclic voltammogram recorded on a graphite electrode at a break potential of –1.6 V (Reference electrode – glassy carbon). Polarization rate – 1 V/s, pure LiCl at 700°C.

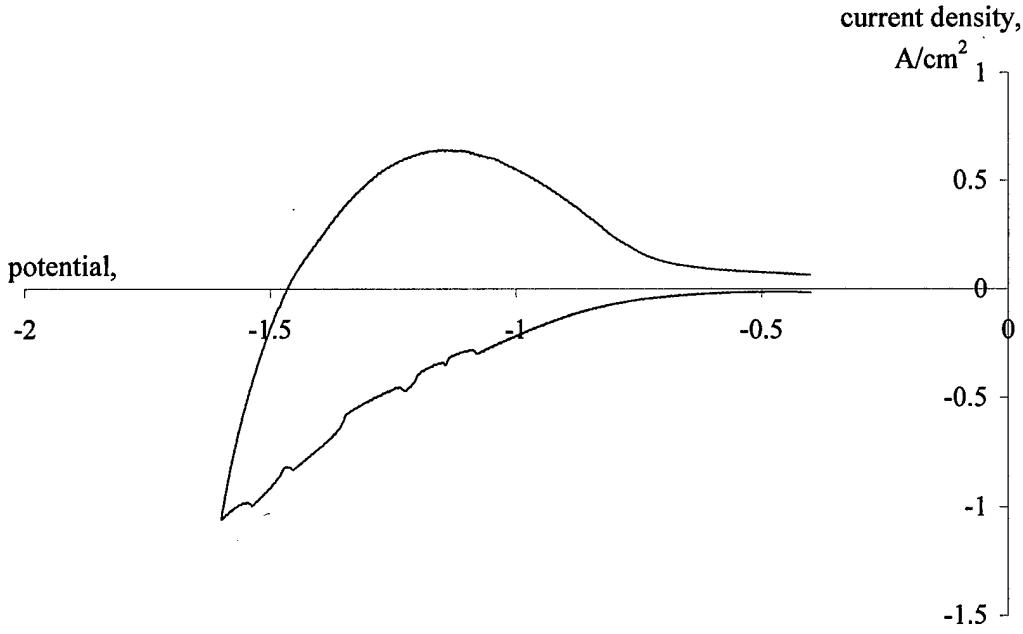

Fig. 17. Cyclic voltammogram recorded on a graphite electrode at a break potential of –1.6 V (Reference electrode – glassy carbon). Polarization rate – 0.1 V/s, pure LiCl at 700°C.

1.3. Discussion

The reversibility of alkali metal deposition/dissolution in a thermodynamic sense is evaluated by us on a 100 % scale by comparing the areas under the anodic and cathodic waves according to the following equation:

$$\mathrm{Rev} = 50 \cdot \left(1 - \frac{A_{anod}}{A_{cathod}}\right), \% \qquad (1)$$

where A_{anod} and A_{cathod} are areas measured under the anodic and cathodic waves of a voltammogram (the area is negative in the cathodic part of the current and positive in the anodic part of the current).

The physical sense of Eq.(1) is clear from considering the following simple cases:

i. when the cathodic and anodic waves are identical, i.e. $A_{cathod} = A_{anod}$, none of the deposited metal was oxidized back, then Rev = 0, meaning that the process is fully irreversible and that all the deposited metal is 'lost';

ii. when the total integral under the anodic wave is zero (i.e. half of it is in the cathodic, while half of it is in the anodic current interval), Rev = 50 %, meaning that half of the deposited metal is 'lost';

iii. when the anodic wave fully compensates the cathodic wave, i.e. $A_{cathod} = -A_{anod}$, Rev = 100 %, the process is fully reversible, meaning that all the deposited metal is oxidized back, i.e. there is no metal 'loss' at all.

In Fig-s 18-20, the reversibility parameter Rev is shown based on the computer analysis of all the curves measured in the sodium chloride melt. From Fig-s 18-20 one can make the following conclusions:

i. for the Mo working electrode the Rev – log v curves have an S-shape form. The majority of curves tend to about Rev = 50 % at $v > 1$ V/s and to about Rev = 0 % at $v < 0.1$ V/s. This behavior can be explained by the fast diffusion of deposited Na into bulk NaCl. When the polarization rate is very slow, almost 100 % of Na is able to escape from the electrode surface, and almost none of the deposited Na is oxidized back in the anodic cycle. However, when the rate of polarization is large, only the part of sodium deposited in the cathodic cycle is 'lost' by diffusion, and the part of sodium deposited in the beginning of the anodic cycle is actually oxidized back in the end of the anodic cycle.

ii. for the GC working electrode the Rev values have approximately the same 50 %, or a bit higher (60 %) value at the largest rate of polarization (20 V/s). However, with decreasing the polarization rate, higher and higher portions of deposited Na are oxidized back, i.e. smaller and smaller amounts of Na are lost into bulk NaCl by diffusion. It is probably due to the adsorption ability of Na to carbon sites. In other words, some kind of a surface NaC_x compound is stable. However, the rate of adsorption is lower than the rate of diffusion into bulk NaCl; that is why the stabilization of deposited Na is enhanced at lower rates of polarization. This enhanced stabilization is clearer from Fig. 21, being the difference of Fig-s 19 and 18.

iii. for the graphite working electrode the Rev values have approximately the same (somewhat larger) values at the largest rate of polarization of 20 V/s, compared to the GC working electrode. Then, at about 3 V/s, the Rev parameter has a maximum value. At this point the Rev parameter on the graphite electrode is significantly larger than on the GC electrode. In other words, the graphite surface has a higher stabilizing ability for Na atoms, compared to the GC surface. It is probably due to the higher roughness, i.e. higher specific surface area of the graphite compared to the GC, ensuring adsorption of the higher amount of Na atoms. However, with decreasing the polarization rate, the Rev

parameter on the graphite electrode sharply decreases towards 0 %, in contrary to what was observed for the glassy carbon electrode. This is obviously due to the diffusion of Na atoms into the graphite phase, and to the stabilization of Na atoms inside graphite by the formation of a stable intercalation compound. This feature is better seen from Fig. 22, being the difference of Fig-s 20 and 19.

Our statements about adsorption and intercalation are supported by the shape and characteristics of the voltammograms shown. In Fig. 1 through 9 a tendency to broadening of the anodic peak as well as its shifting towards more positive values of potential is observed as we move from the molybdenum to the glassy carbon and then further to the graphite electrode. Usually such behavior takes place when adsorption/compound formation is involved in the reduction process. So the shape and parameters of the voltammetric curves presented may be evidence that adsorption in the case of glassy carbon and adsorption/intercalation in the case of graphite electrode play an important role in the reduction process of sodium.

From the comparison of Fig-s 18-22, one can conclude that the rates of the three competitive processes can be presented in the following order:

i. the fastest is the diffusion of Na into NaCl, probably due to the special electron-jump mechanism;
ii. adsorption of Na on the carbon sites has an intermediate rate;
iii. the slowest is the diffusion of sodium into graphite with the formation of the intercalation compound.

The reversibility parameter Rev calculated for the voltammograms taken in the lithium chloride melt on the 3 electrodes is shown in Figs. 23-25. The following conclusions can be made:

i. in the case of the steel electrode parameter Rev has a value of 65-75% at a polarization rate of 20 V/s. However, at lower polarization rates the value of reversibility depends strongly on the break potential. Thus, for –2.0 V we have Rev = 15.89 %, while for –2.2 V the value of reversibility is 78.81 %. Further experiments are needed to understand this phenomenon;
ii. for the glassy carbon electrode we have the value of parameter Rev of around 55 % at a polarization rate of 20 V/s, while at 0.03 V/s the reversibility of lithium reduction is 75-85 %. This phenomenon can be explained in terms of adsorption of lithium atoms to the electrode surface with the formation of a LiC_x surface compound, i.e. it is similar to what was observed in the case of sodium, which is supported by the presence of broad anodic peaks in the voltammograms;
iii. for the graphite cathode parameter Rev for the majority of curves is 80-90%, which is higher than for the glassy carbon electrode, and can be explained by a higher stabilizing ability of graphite for lithium, compared to glassy carbon, i.e. in the same manner as it was done for sodium. Unlike in the case of sodium, there is no "drop" in reversibility at low polarization rates (that is, below 3 V/s). We explain this by the fact that lithium has a significantly smaller atomic radius than sodium (1.55 Å for lithium and 1.89 Å for sodium, respectively). Lithium atoms intercalated between the graphite planes (the distance between the latter is 3.35 Å) can freely move back out of graphite and be oxidized electrochemically when electrode polarization is reversed. However, sodium atoms once intercalated cannot come out easily from the graphite structure. As it was pointed out above, the more metal deposited on the electrode is oxidized back electrochemically, the higher the reversibility of the process is. So more lithium is oxidized in the anodic cycle of the voltammograms compared to sodium, which gives rise to the values of reversibility at polarization rates below 3 V/s.

In the future, we are going to develop a quantitative model of the processes described above, and thus to quantify the rates of diffusion and adsorption/desorption of Na and Li, including the rate of their intercalation into graphite. Although qualitatively, but we were able to 'catch' the fingerprint of sodium and lithium intercalation into graphite in the figures shown in this section

(especially in Fig. 22 in its low polarization rate part), which, as commonly accepted, is the first and the key step of carbon nano-tube formation.

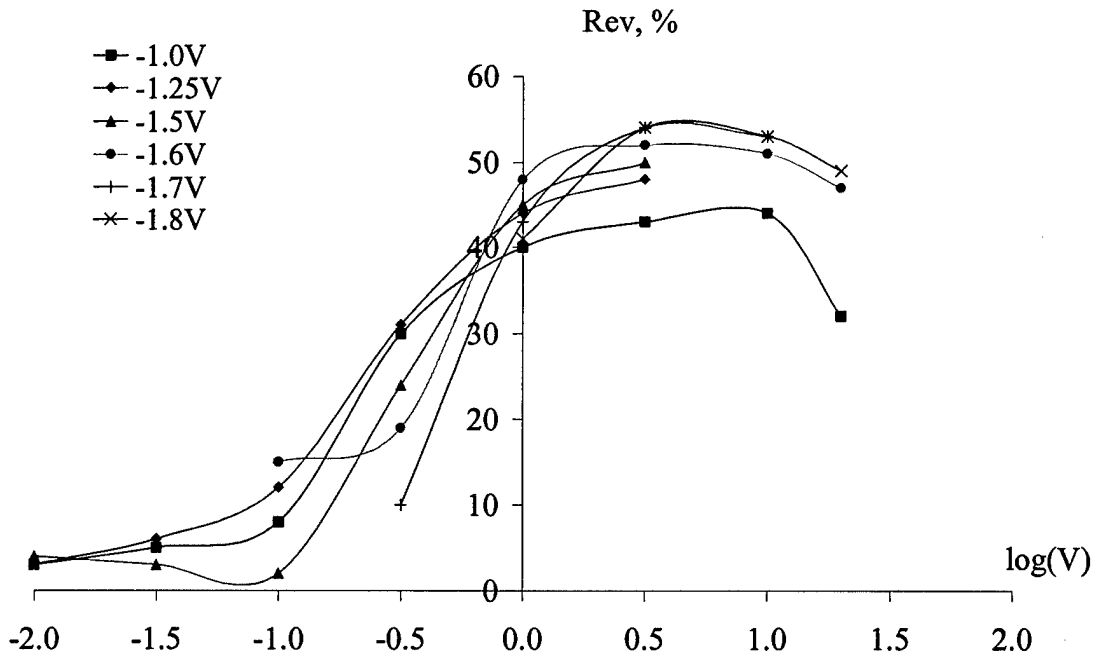

Fig. 18. Reversibility parameter Rev as a function of polarization rate (semi-logarithmic scale) at different break potentials (Reference electrode - Mo) measured on a Mo electrode in pure NaCl at 850°C.

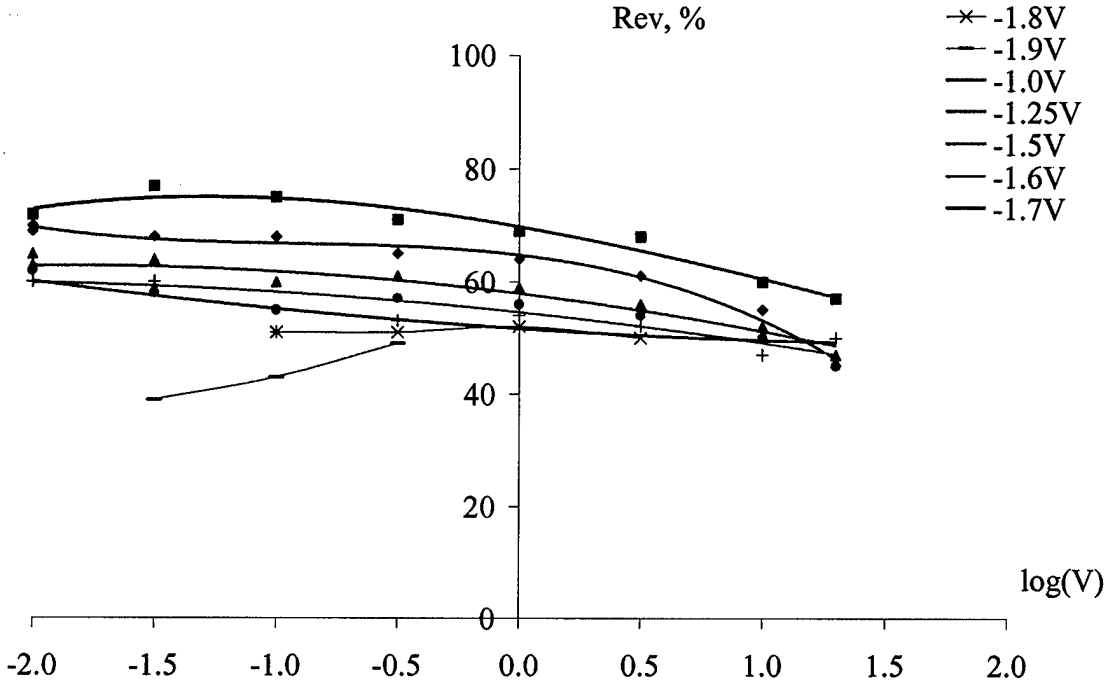

Fig. 19. Reversibility parameter Rev as a function of polarization rate (semi-logarithmic scale) at different break potentials (Reference electrode - Mo) measured on a GC electrode in pure NaCl at 850°C.

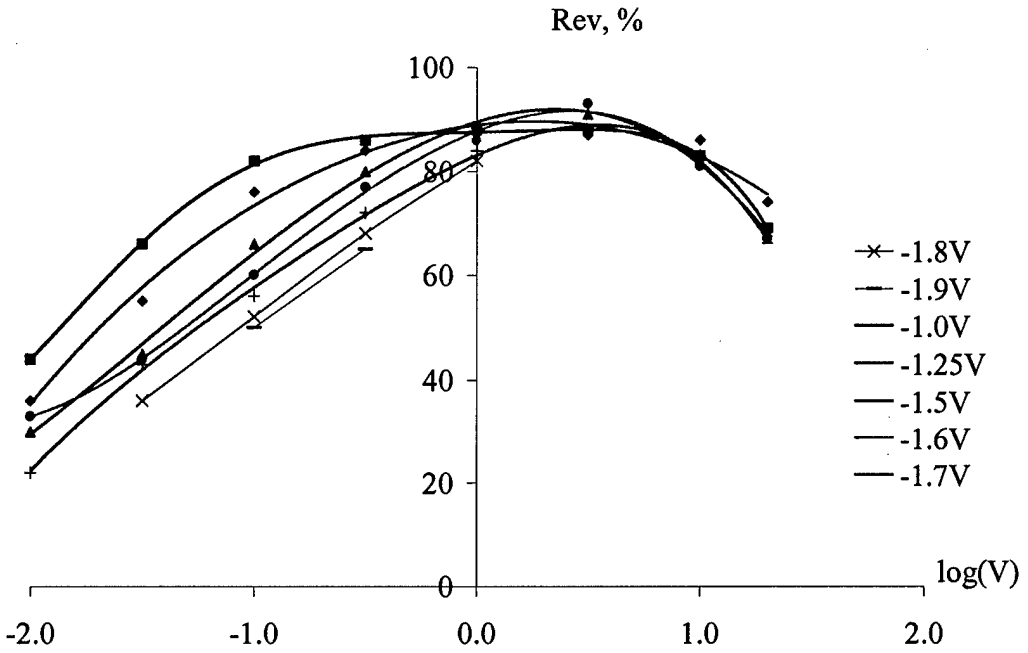

Fig. 20. Reversibility parameter Rev as a function of polarization rate (semi-logarithmic scale) at different break potentials (Reference electrode - Mo) measured on a graphite electrode in pure NaCl at 850°C.

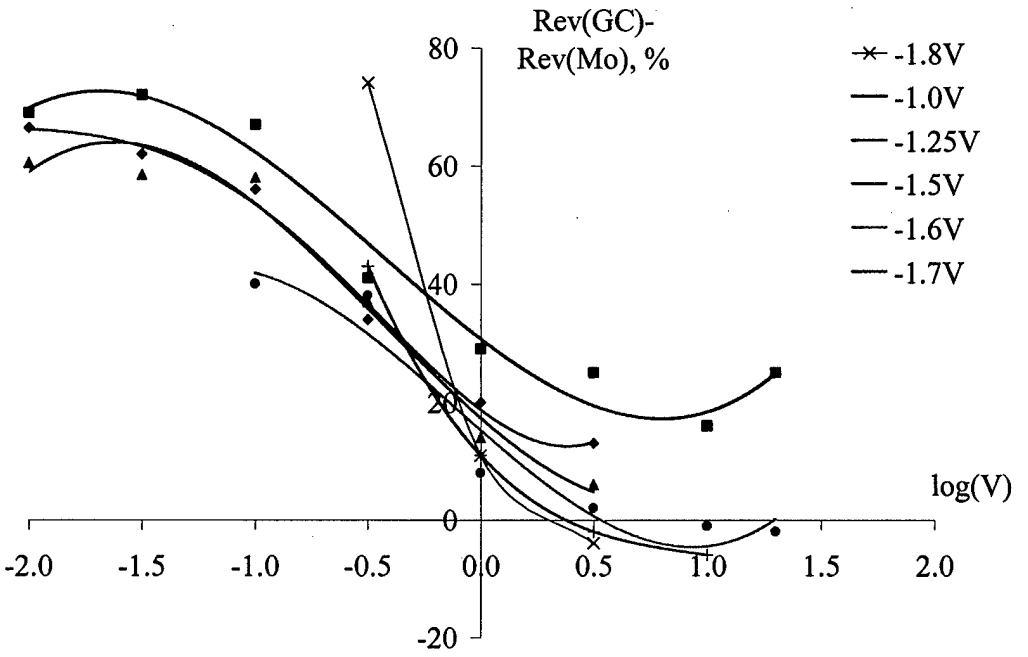

Fig. 21. The difference of reversibility parameters Rev between GC and Mo working electrodes (i.e. difference of Fig-s. 19 and 18).

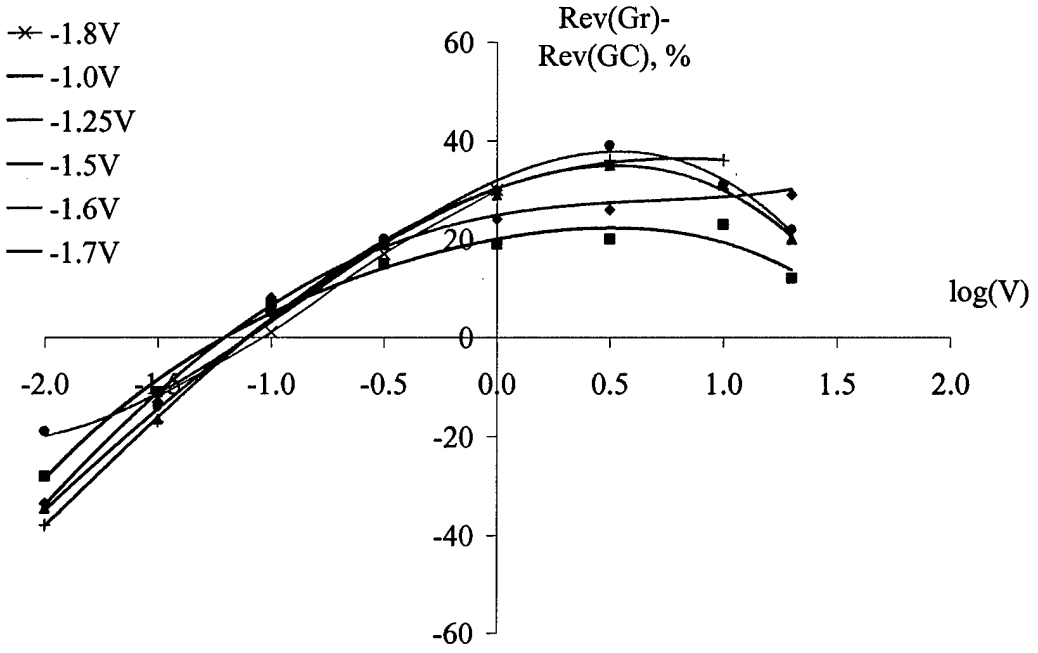

Fig. 22. The difference of reversibility parameters Rev between graphite (Gr) and GC working electrodes (i.e. difference of Fig-s. 20 and 19).

Fig. 23. Reversibility parameter Rev as a function of polarization rate (semi-logarithmic scale) at

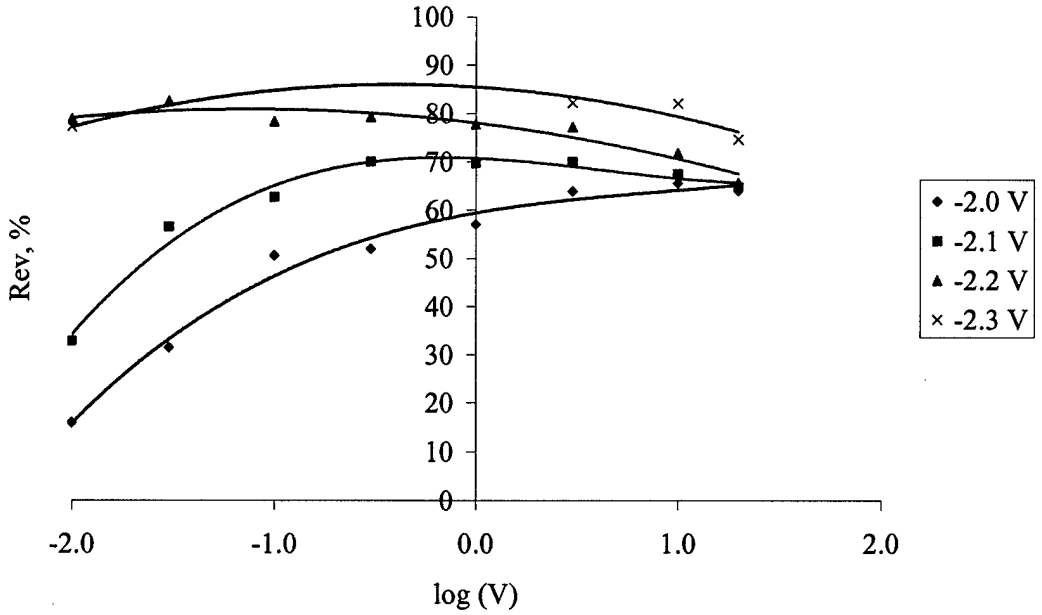

different break potentials (Reference electrode – glassy carbon) measured on a steel electrode in pure LiCl at 700°C.

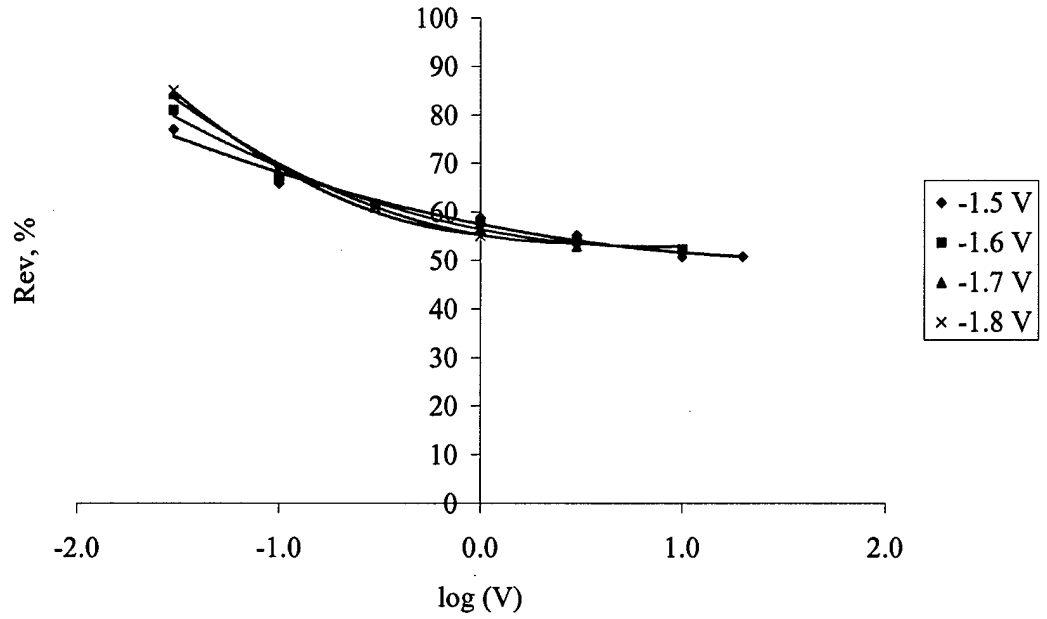

Fig. 24. Reversibility parameter Rev as a function of polarization rate (semi-logarithmic scale) at different break potentials (Reference electrode – glassy carbon) measured on a glassy carbon electrode in pure LiCl at 700°C.

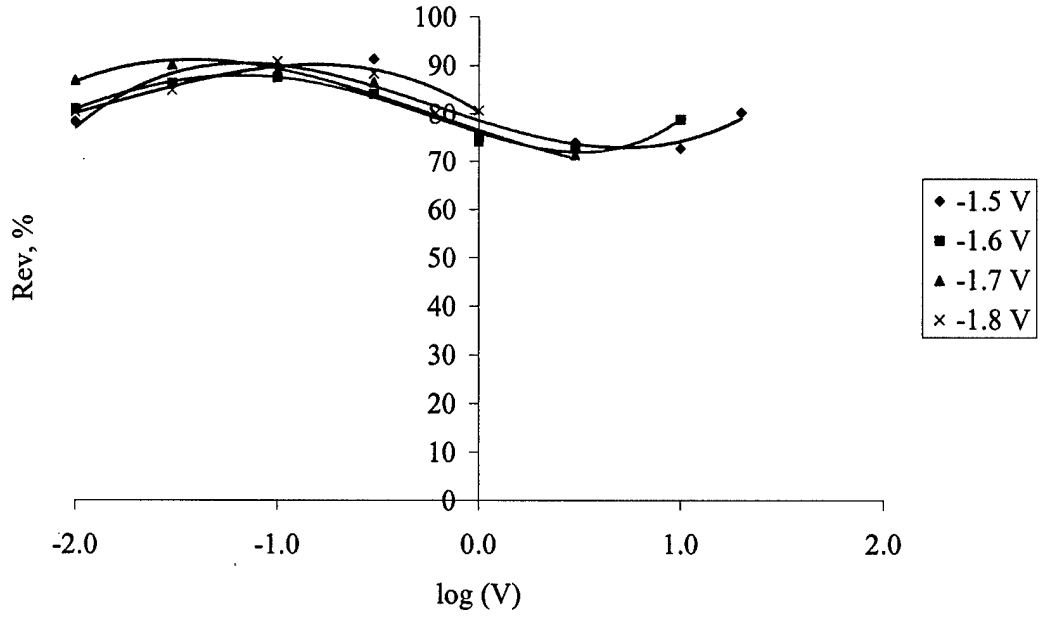

Fig. 25. Reversibility parameter Rev as a function of polarization rate (semi-logarithmic scale) at different break potentials (Reference electrode – glassy carbon) measured on a graphite electrode in pure LiCl at 700°C.

The goal of this part of the work is to 'go straight ahead', performing electrolysis experiments under different conditions and to analyze the product, mainly from the point of view of the carbon tubes formed, in the nanometer–micrometer interval of their diameter.

2.1. Experimental

2.1.1. Procedure

Several types of electrolytes were used to produce carbon nano/micro-tubes: pure $CaCl_2$, $CaCl_2$-$MgCl_2$(1 mol. %), NaCl-$MgCl_2$(5 mol. %), NaCl-KCl-$MgCl_2$(5 mol. %). The salts were dried in an electric furnace under vacuum at 120°C for 40 hours. The electrolyte was then melted in a glassy carbon crucible under pure, dry argon atmosphere. The working temperature for all the electrolytes used was 850°C. A graphite cathode and glassy carbon reference electrode were immersed into the melt and it was electrolyzed at –1.9 V for 15 min. ($CaCl_2$), at –1.4 V for 15 min. ($CaCl_2$-$MgCl_2$), at –1.1 V for 10 min. (NaCl-$MgCl_2$), and at –1.3 V for 15 min. (NaCl-KCl-$MgCl_2$). All the potentials were measured versus the potential of the glassy carbon reference electrode. For the three magnesium-containing melts, the electrolysis potential was chosen so that only magnesium was deposited on the cathode.

Pure lithium chloride was used as well to obtain carbon nano-tubes. The salt was carefully dried in vacuum at 120°C for 40 h. Then the temperature was raised up to 500°C and the system was kept at these conditions for an hour being flushed periodically with pure dry argon. The same procedure was repeated at 600°C. After that the system was filled with argon and heated up to 700°C. Two different electrolysis experiments have been performed in the LiCl melt. In experiment 1, eighty-one voltammetric curves were taken fist to study the mechanism of lithium reduction using graphite working and glassy carbon reference electrode (see Chapter 1 for details). After that we performed electrolysis at a constant current of 900 mA for 20 min. using the same working electrode and recording changes of the electrode potential in time. In experiment 2 the electrolysis at the same conditions (900 mA/20 min.) was started right after the salt was melted.

As a result, the originally white salts turned into gray. After cooling the system to room temperature, the carbonaceous material was carefully separated from the frozen salt and analyzed by Scanning Electron Microscopy (SEM) and Atomic Force Microscopy (AFM). Carbon nano/micro-structures with various diameters, lengths and shapes have been found in the electrolyte as well as on the cathode surface.

2.1.2. Sample preparation

Two different techniques were used for the preparation of samples for the analysis.

The $CaCl_2$, $CaCl_2$-$MgCl_2$(1 mol. %) and LiCl samples after cooling down were dissolved in hot distilled water. The carbon containing compounds were extracted with toluene and sonicated in acetone for 10 minutes. Activated in HF and 3-aminopropyl-methil-diethoxi-silane silicon single crystal chips were sonicated in the dispersions to produce samples for AFM.

To prepare the NaCl-$MgCl_2$(5 mol. %) and NaCl-KCl-$MgCl_2$(5 mol. %) samples, a dialysis-based cleaning method was performed. Schematic view of the cleaning setup is shown in Fig. 15.

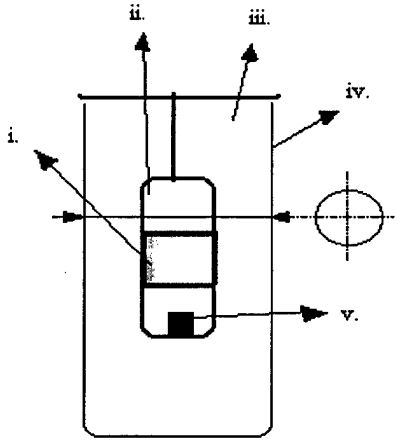

Fig. 15. Schematic view of the cleaning setup.
i.-membrane, ii.-inner diffusion space, iii.-outer diffusion space,
iv.-vessel, v.-solidified salt to be cleaned.

The solidified sample was placed in the inner diffusion space with a membrane, and the system was filled with distilled water. The water in the outer zone was changed every day until the concentration of Na^+-ions was close to zero. Fig. 16 shows the concentration dependence of Na^+ on time (measured by flame photometry method).

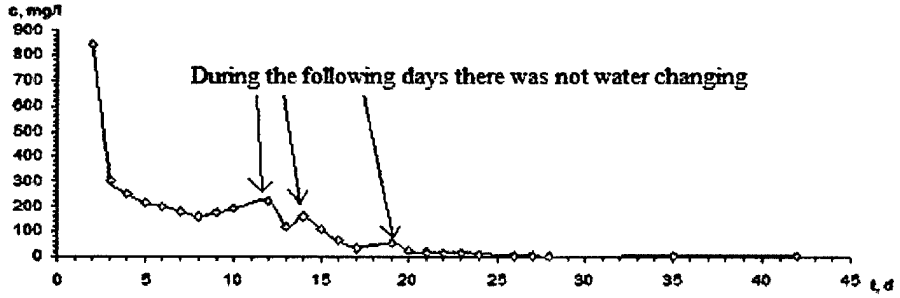

Fig. 16. Concentration of Na^+ as a function of time during the cleaning period.

After that small parts of the suspension (1-1.5 ml in volume) were mixed with 6-8 ml of hydrochloric acid, acetone, toluene and distilled water respectively, and then the four mixtures were treated by ultrasound for 6•15 min. After that a small "drop" was taken from the sediment and put onto an aluminum plate, dried and covered with a gold layer.

2.2. Results and discussion

AFM images of a tube-like structure found in the $CaCl_2$-$MgCl_2$(1 mol. %) sample with the results of cross-section analysis are shown in Fig. 17 through 20. It can be seen that this structure is 1000-1100 nm long and 3.5-4 nm in diameter.

SEM image of a carbon micro-tube found in the NaCl-$MgCl_2$(5 mol. %) sample is presented in Fig. 21. One can see that the diameter of the tube in Fig. 21 is about 1 μm. Unfortunately, it is impossible to evaluate the tube length because only a part of it is visible.

SEM image of the cathode surface after electrolysis in the NaCl-KCl-$MgCl_2$(5 mol. %) melt is shown in Fig. 22. A tube-like structure with a diameter of about 0.5 μm and 2 μm long can be seen at the center of the image. The results of EDAX ZAF elemental analysis show that it is almost pure carbon (Table 1).

It was mentioned above that, according to our present understanding, nano/micro-tubes are formed in the bulk of the melt from the graphite plates ablated by alkali or alkaline earth metal atoms intercalating into the graphite structure. The image in Fig. 22 may be evidence that tube formation can take place on the cathode surface as well. We think that "partial" ablation of graphite plates when only part of the plate is off the electrode surface may also occur. When the dimensions of such a plate are big enough for it to bend, a tube-like structure is formed.

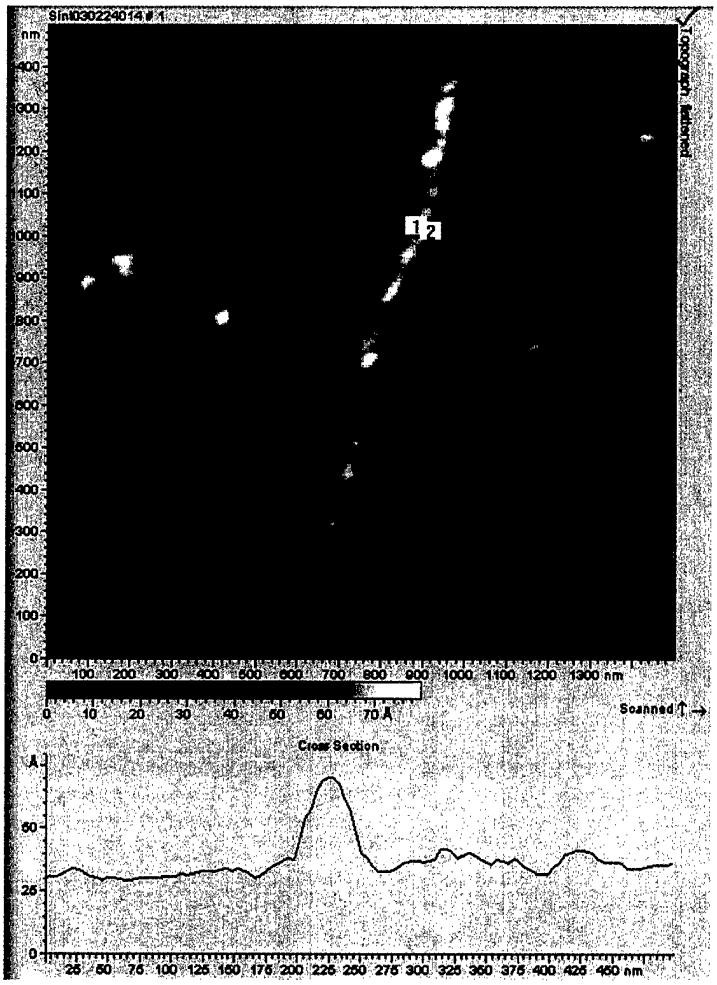

Fig. 17. AFM image of a tube-like structure with a cross-section obtained in the $CaCl_2$-$MgCl_2$ sample.

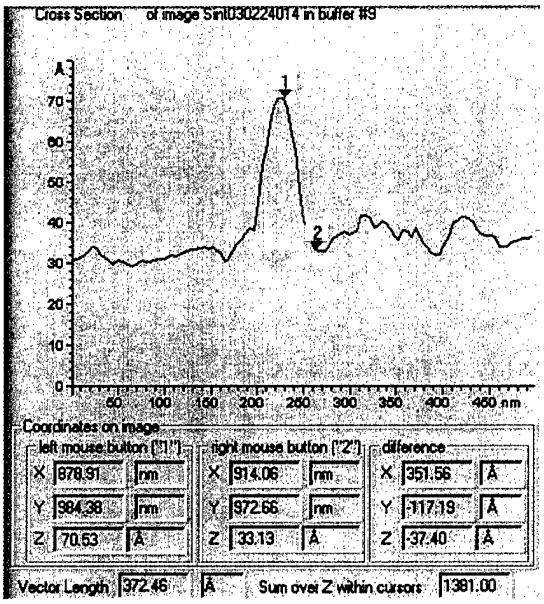

Fig. 18. Results of analysis of the cross-section in the AFM image shown above.

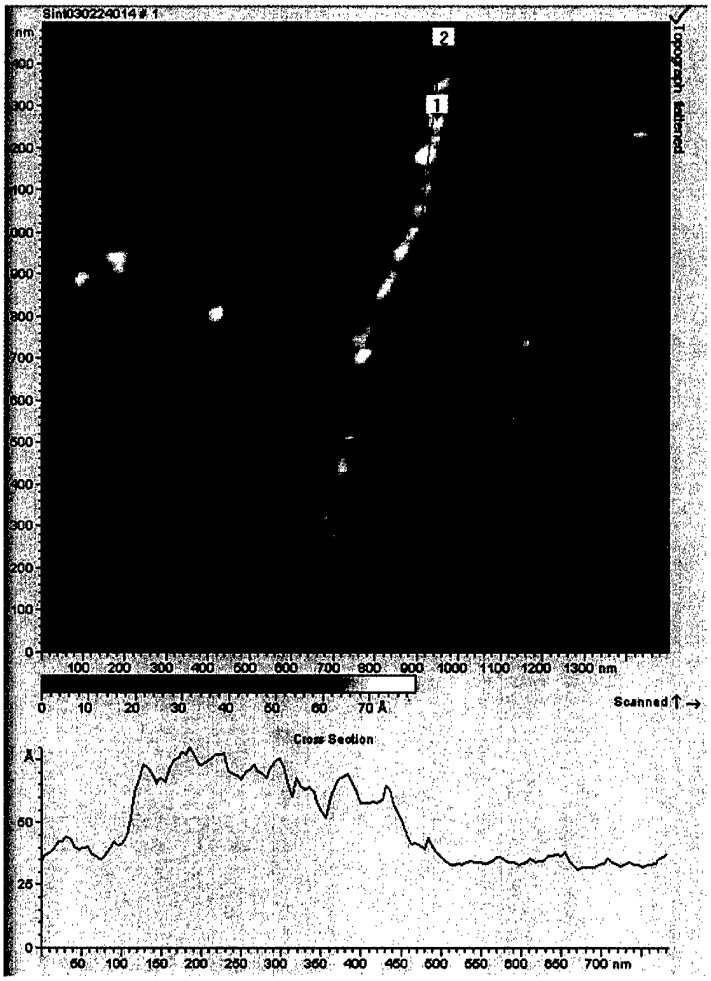

Fig. 19. AFM image of the tube-like structure with another cross-section obtained in the $CaCl_2$-$MgCl_2$ sample.

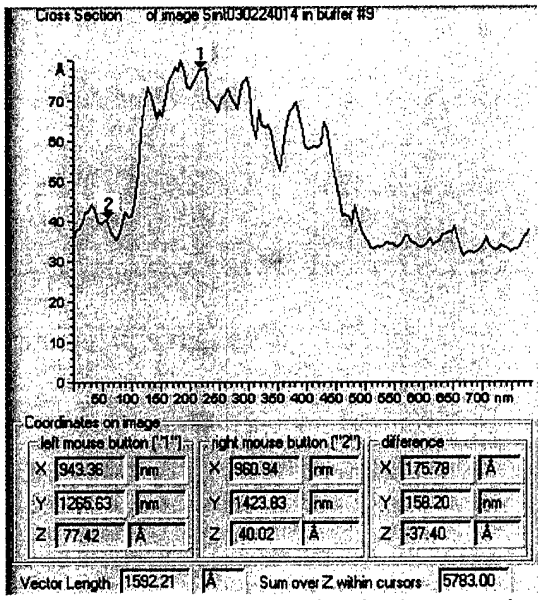

Fig. 20. Results of analysis of the cross-section in the AFM image shown above.

Fig. 21. SEM image of a carbon micro-tube with a diameter of about 1 μm for the case of the NaCl-$MgCl_2$(5 mol. %) molten system. The tube was found in the frozen electrolyte.

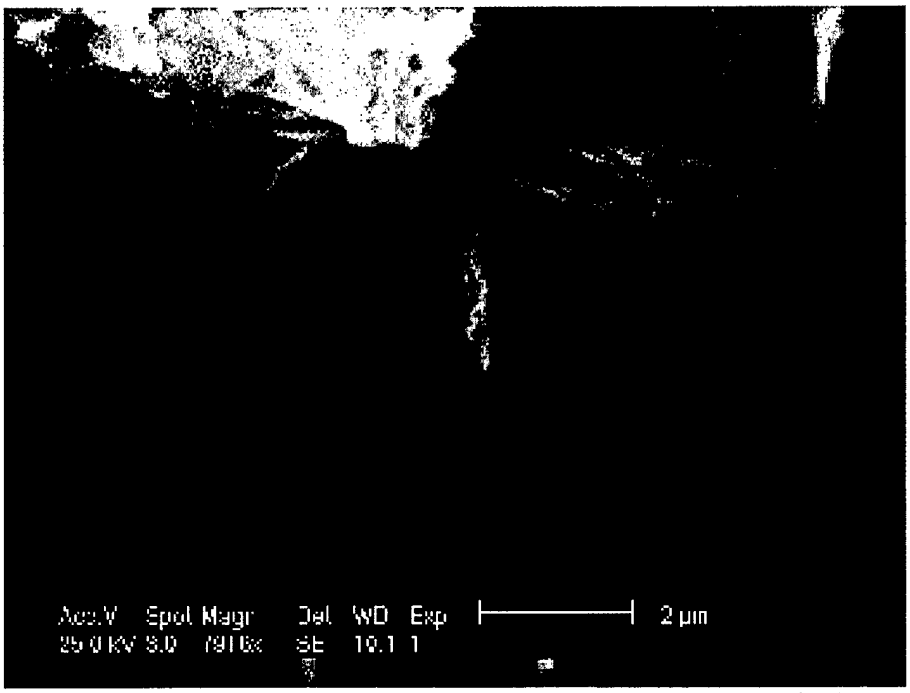

Fig. 22. SEM image of a carbon micro-tube grown on the cathode surface in the case of the NaCl-KCl-$MgCl_2$(5 mol. %) melt.

Table 1. EDAX ZAF Quantification (Standardless)
Element Normalized

Element	Wt. %	At. %
C*K*	96.13	98.78
Mg*K*	1.04	0.53
Cl*K*	0.53	0.19
Fe*K*	2.29	0.51
Total	100.00	100.00

The potential – time curves for the electrolysis experiments in the LiCl melt are shown in Figs. 23, 24. One can see that there are sharp and rather random changes of the electrode potential in curve 1 and in the beginning of curve 2, which can be evidence that ablation of graphite planes leading to changes in the electrode surface takes place. The electrolysis in experiment 2 was interrupted in the 18th minute due to overpotential (the value of electrode potential went beyond –15 V allowed by the potentiostat). It could happen if the electrode material (graphite) being in the electrolyte and at the electrolyte/gas interface eroded completely causing the electric circuit to break, which is confirmed by almost twofold decrease in the electrode mass (from 0.2209 g to 0.1348 g).

SEM images taken from the samples obtained in the two experiments with lithium chloride are shown in Figs. 25-27. It should be pointed out that in this case no tubes or tube-like structures were found on the electrode surface but in the solidified electrolyte. It can be seen that the diameter of tubes in Fig. 25 (experiment 1) is around 50 nm, while in Figs. 26-27 (experiment 2) it is about 150 nm. We mentioned above that in experiment 1 the electrolysis began after taking a large number of voltammograms, so the electrolyte could be saturated with lithium metal (or at least contain a certain amount of it) prior to the electrolysis and lithium metal influenced the tubes diameter. However, further experiments are needed to clarify if alkali metal (Li, Na) dissolved in its chloride has any influence on the tube diameter. As it was in the case of the NaCl-$MgCl_2$(5 mol. %) sample, it is impossible to evaluate the tube length because the tubes

are twisted and visible only partly. According to EDAX ZAF elemental analysis, the tubes are composed mainly of carbon and contain some undissolved salt.

The two samples were analyzed by the AFM method as well but no tubes with diameters below 50 nm were found.

It is still unclear how the electrolyte chemistry and electrolysis parameters influence the dimensions of the tubes formed. On the other hand, the mechanism of tubes formation is far from being fully studied and understood. So further work, both concerning fundamental and applied aspects of nano/micro-tubes formation, is needed in order to find electrolyte compositions as well as electrolysis conditions optimal for the tubes production.

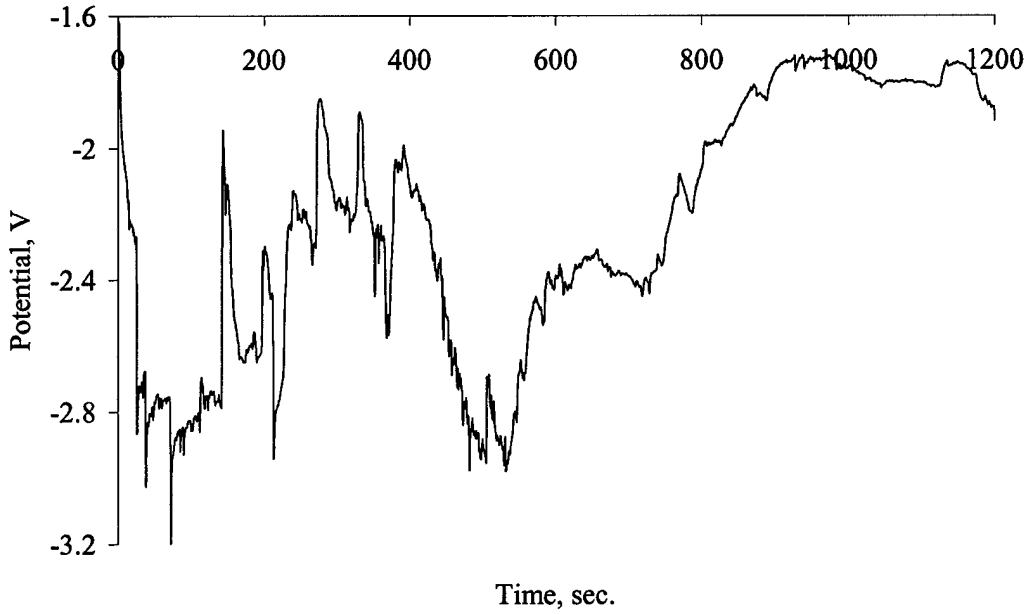

Fig. 23. Chronopotentiogram of the electrolysis experiment 1 in the LiCl melt. Current - 900 mA, time – 20 min., T= 973 K.

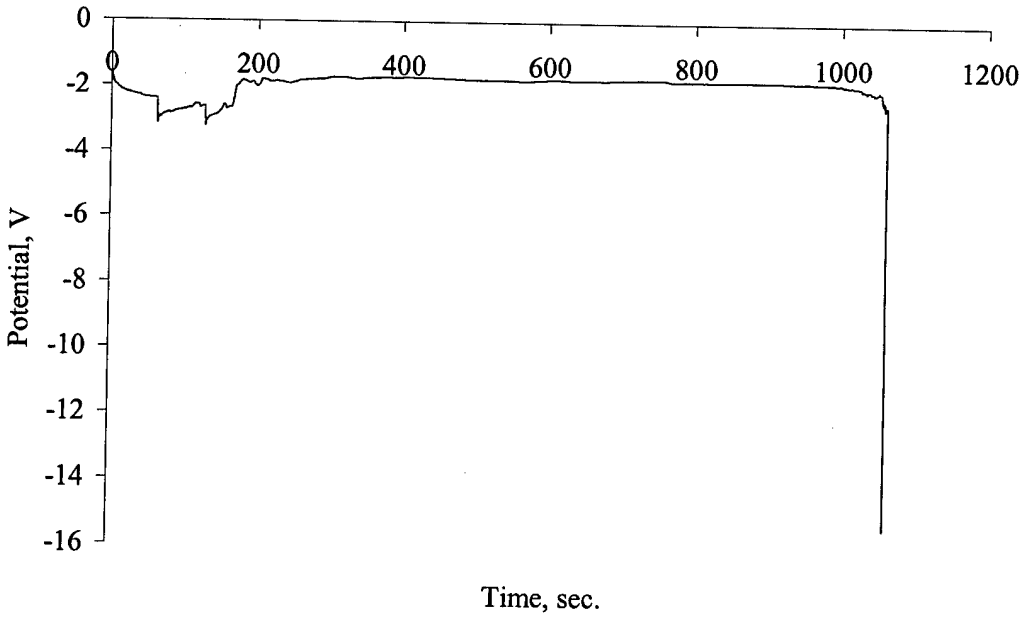

Fig. 24. Chronopotentiogram of the electrolysis experiment 2 in the LiCl melt. Current - 900 mA, time (planned) – 20 min., T= 973 K.

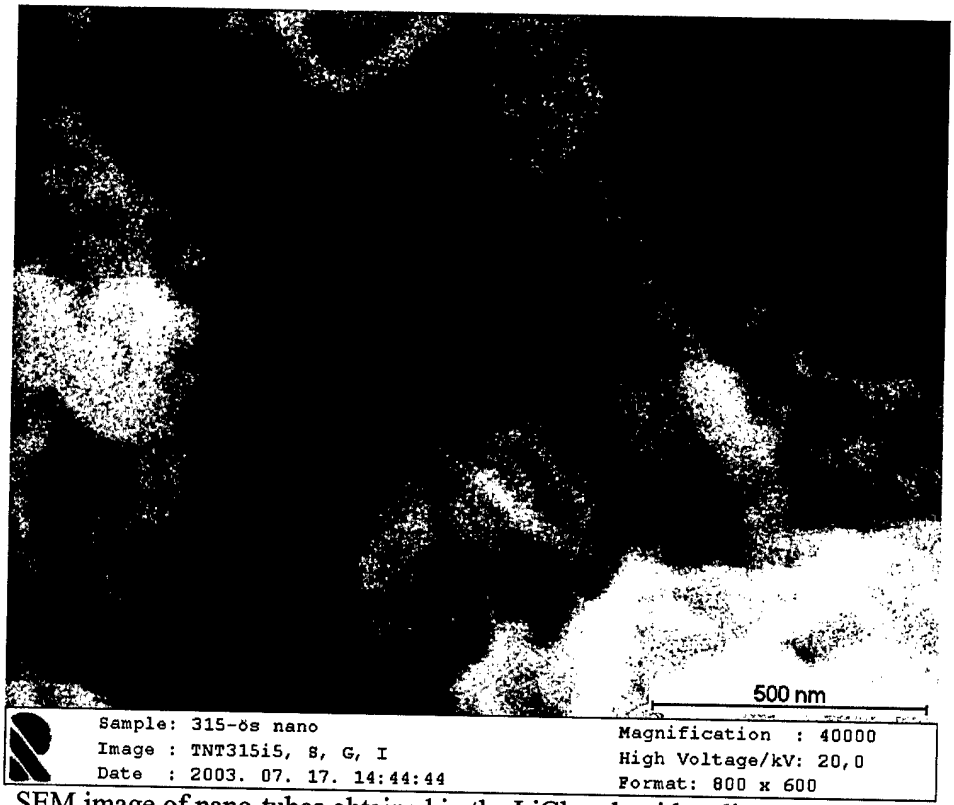

Fig. 25. SEM image of nano-tubes obtained in the LiCl melt with a diameter of around 50 nm (experiment 1). The tubes were found in the bulk of the electrolyte.

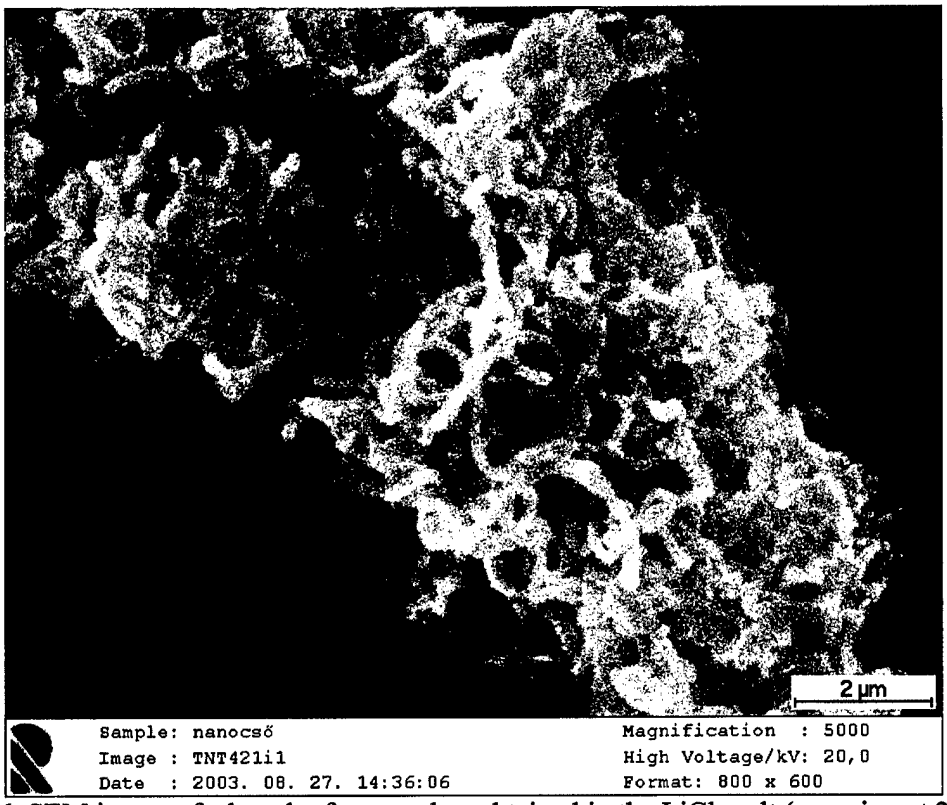

Fig. 26. SEM image of a bunch of nano-tubes obtained in the LiCl melt (experiment 2). The tubes were found in the bulk of the electrolyte.

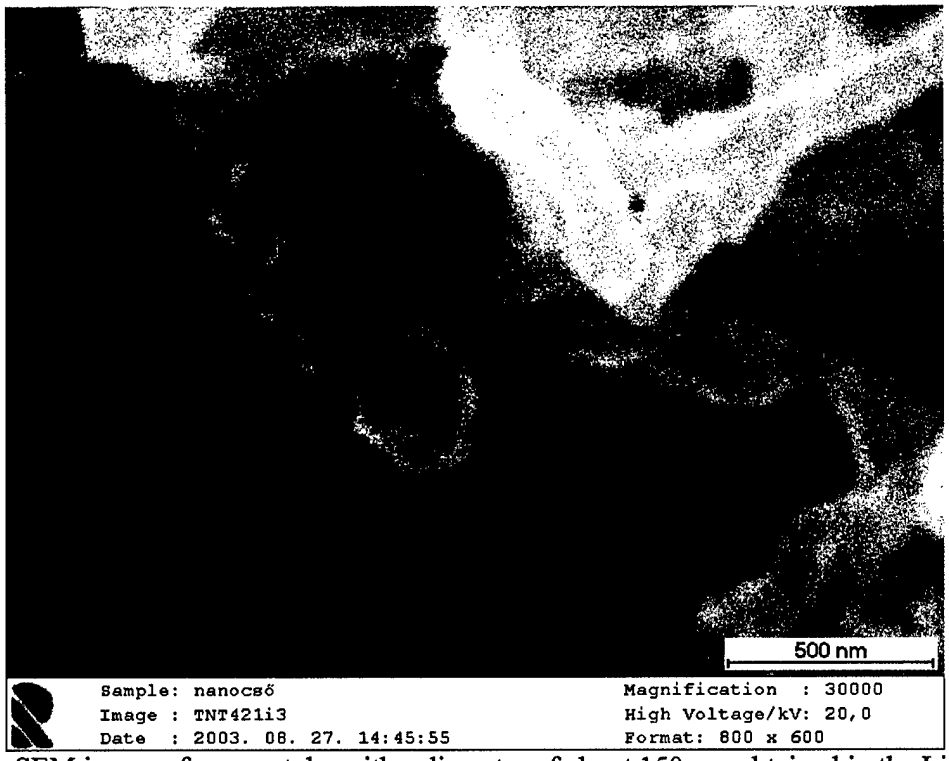

Fig. 27. SEM image of a nano-tube with a diameter of about 150 nm obtained in the LiCl melt (experiment 2). The tube was found in the bulk of the electrolyte.